Ambidextrous optically active copper(II) phthalocyanine supramolecules induced by peripheral group homochirality†

Wei Zhang,*[ab] Akira Ishimaru,‡[a] Hisanari Onouchi,§[a] Roopali Rai,¶[a] Anubhav Saxena,¶[a] Akihiro Ohira,‖[a] Masaaki Ishikawa,[a] Masanobu Naito[a] and Michiya Fujiki*[a]**

Received (in Montpellier, France) 18th May 2010, Accepted 18th June 2010
DOI: 10.1039/c0nj00374c

Self-assembling features of the disk-shaped copper(II) phthalocyanine (Pc) molecules carrying four enantiopure (*S*)- and (*R*)-1-(*p*-tolyl)ethylaminocarbonyl groups at their peripheral positions, CuPc-(*S*) and CuPc-(*R*), were studied. For comparison, an analogous CuPc carrying racemic 1-(*p*-tolyl)ethylaminocarbonyl groups, CuPc-(*RS*), was used. From circular dichroism and visible/infrared spectroscopic studies with wide-angle-X-ray diffraction data, CuPc-(*S*) and CuPc-(*R*) were shown to generate optically active $\pi-\pi$ stacked assemblies formed in less-polar solvents. CuPc-(*RS*) produced similar assemblies with a loss of optical activity in the less-polar solvents. Plural interactions of Pcπ/Pcπ stacking, quadruple hydrogen bonding, homochiral stereocenters at the peripheral groups, bulky aralkyl entities and weak coordinating nature of copper(II) of the CuPcs were thought to be responsible for the formation of the optically active CuPc assemblies. The solvent effect was evident: less polar chloroform and tetrahydrofuran helped to generate the optically active CuPc assembly while highly polar *N*,*N*-dimethylformamide gave a monomeric Pc species due to the loss of Pc–Pc intermolecular hydrogen-bonding interaction. The self-assembling ability of the CuPcs was similar to NiPc analogues carrying the same chiral peripherals reported previously. Atomic force microscope study revealed that by casting dilute chloroform solutions of CuPc-(*S*), CuPc-(*R*) and CuPc-(*RS*) onto mica surface, worm-like supramolecular polymers were observed while the NiPc-(*R*) analogue provided needle-like supramolecular polymers.

Introduction

DNA and polypeptide, which are typical biopolymers, consist of D-ribose and L-amino acid as chiral building blocks with the same handedness, respectively. Scientists have long thought about the origin of biomolecular homochirality. Due to biomolecular handedness, biopolymers are able to adopt inherent helical and suprahelical architectures in water.[1] The enantiopurity is responsible for the emergence of many biological functions involving enzymatic catalysis, heritable characters, and pharmaceutical and toxicological activities.

From the viewpoint of polymer chemistry and supramolecular chemistry, double-strand (ds) stiff DNA chain is classified into a supramolecular polymer made of two single-strand (ss) flexible DNA chains with the help of hydrogen-bonding, $\pi-\pi$ and electrostatic interactions. The backbone of ss-DNA is a floppy alternating copolymer made of enantiopure deoxynucleoside and achiral phosphate moiety. Deoxynucleoside is a monomer composed of D-ribose bearing four different achiral π-conjugated nucleobases (adenine, cytosine, guanine, and thymine). As the $\pi-\pi$ stacks of nucleobases are slippery, twist sense of the helical motif is induced by the D-ribose homochirality. The nucleobase $\pi-\pi$ stacking structures are hence covalently linked by achiral phosphate.

By learning this programmed left–right preference in biological chirality, the self-organisation of artificial synthetic molecules to design supramolecular materials with novel functions has been widely exploited.[2,3] Among these, several π-conjugated molecules involving triphenylene, porphyrin and phthalocyanine (Pc) have been widely investigated as building blocks for key materials to produce molecule-based electronic, photonic and optoelectronic devices.[4,5]

Pc and its metal derivatives (MPcs) among π-conjugated molecules have received much attention due to their high thermal and chemical stability, chemical modification ability, photoconductivity in visible region and dark conductivity upon doping.[6,7] As one of the most interesting structure–property relationships in the field of Pc-related material science, several optically active Pcs and MPcs which are able to adopt one-dimensional (1-D) helical architectures are successfully generated due to their high cofacially $\pi-\pi$ stacking

---

[a] *Graduate School of Materials Science, Nara Institute of Science and Technology, 8916-5 Takayama, Ikoma, Nara 630-0192, Japan. E-mail: fujikim@ms.naist.jp; Tel: +81 743-72-6040*
[b] *College of Chemistry, Chemical Engineering and Materials Science of Soochow (Suzhou) University, Suzhou 215123, China. E-mail: weizhang@ms.naist.jp, weizhang@suda.edu.cn*

† Electronic supplementary information (ESI) available: MALDI-TOF mass and IR spectra of CuPc-(*S*), CuPc-(*R*) and CuPc(*RS*), CD/visible spectra of CuPc-(*S*) in DMF and CD/visible spectra of CuPc-(*S*) in $CHCl_3$. Preliminary VSM data of CuPc-(*R*), EPR spectrum of CuPc-(*S*), and AFM and MFM data of CuPc-(*S*) on mica. See DOI: 10.1039/c0nj00374c

‡ Current address: Stella Chemifa Corporation, Japan.

§ Current address: Nitto Denko Corporation, Japan.

¶ Current address: GE India Technology Centre, Bangalore, India.

‖ Current address: Advanced Industrial Science and Technology (AIST), Japan.

** Current address: JASCO Corporation, Japan.

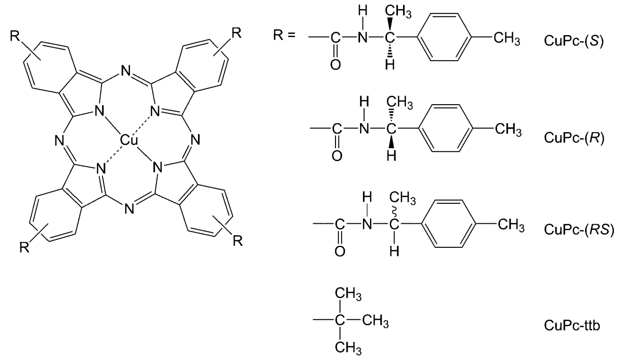

Chart 1 Chemical structures of CuPc-(*S*), CuPc-(*R*), CuPc-(*RS*) and CuPc-ttb.

ability. Several workers have reported facile generation of helical Pc and MPc supramolecules so far.

In 1999, Nolte *et al.* first demonstrated the generation of optically active helical polymer and supramolecules by self-assembling Pc molecules bearing chiral alkyl side groups.[1b,8] Kimura *et al.* recently reported the self-organisation behavior of optically active Pc dimers and MPcs (M = Zn and Co) carrying branched alkyl chains with hydrogen-bonding OH groups.[4d] Liu *et al.* successfully prepared optically active Pc–polysiloxane from achiral Pc monomers as the starting building block.[7d] We previously reported two soluble nickel(II) Pcs carrying enantiopure (*S*)- and (*R*)-1-(*p*-tolyl)-ethylaminocarbonyl groups at their peripheral positions, PcNi-(*S*) and PcNi-(*R*), respectively, allowing to spontaneously generate optically active 1-D self-assembled hyperhelical supramolecular structure by casting its dilute solution onto solid mica surface under controlled manner.[9] However, a relationship between Pc building block, cavity metal, and assembling nature with a preferential handedness remains unclear.

Herein we report the optically active self-assembling feature of copper(II) Pc molecules carrying four enantiopure (*S*)- and (*R*)-1-(*p*-tolyl)ethylaminocarbonyl groups at their peripheral positions, CuPc-(*S*) and CuPc-(*R*), as shown in Chart 1. For comparison, CuPc-(*RS*) carrying a racemic mixture of four *p*-tolylethylaminocarbonyl groups and CuPc-ttb carrying four *tert*-butyl groups were studied. Although CuPc-(*S*) and CuPc-(*R*) are analogous compounds of the corresponding NiPc-(*S*) and NiPc-(*R*), the self-assembling behaviours of the two CuPcs were much different though subtle differences exist between Cu(II) and Ni(II).

Experimental section

Materials

All the solvents for circular dichroism (CD) and UV measurements were spectroscopic grade and used as received without further purification. 4(5),4′(5′),4″(5″),4‴(5‴)-Tetracarboxyphthalocyaninato copper(II) (Wako), $SOCl_2$ (Wako), triethylamine (Wako), and (*S*)-, (*R*)-, and (*RS*)-1-(*p*-tolyl)ethylamines (TCI) ($[\alpha]_D^{20}$ = −35 to −39 (neat) for the (*S*)-isomer and $[\alpha]_D^{20}$ = +35° to +39 (neat) for the (*R*)-isomer, according to TCI catalogue) were used as received. Copper(II) 4(5),4′(5′),4″(5″),4‴(5‴)-tetrakis(1-(*S*)-(*p*-tolyl)ethylaminocarbonyl)phthalocyanine, CuPc-(*S*), copper(II) 4(5),4′(5′), 4″(5″),4‴(5‴)-tetrakis(1-(*p*-tolyl)ethylaminocarbonyl)phthalocyanine, CuPc-(*RS*), and 4(5),4′(5′), 4″(5″),4‴(5‴)-tetrakis-(1-(*R*)-(*p*-tolyl)ethylaminocarbonyl)phthalocyanine, CuPc-(*R*), were prepared according to our method reported previously.[9] For comparison, as soluble Cu(II)Pc analogue without aralkyl amide peripheral groups, copper(II) 4(5),4′(5′),4″(5″),4‴(5‴)-tetra-*tert*-butylphthalocyanine prepared previously[6f] and NiPc-(*S*) prepared previously were used.[9]

Measurements

CD and visible-near infrared absorption spectra were recorded on a JASCO J-725 spectropolarimeter and JASCO V-570/V-550 spectrophotometers, respectively. IR spectra (32 time scans, 4 cm^{-1} in resolution) were obtained on a Horiba FT-730 FT-IR spectrometer. MALDI-TOF MS spectra were obtained with a Perseptive Biosystems Voyager DE-STR with dithranol (Aldrich) as a matrix in linear mode. Atomic force microscope (AFM) imaging was conducted on a Veeco Nanoscope IIIa with a tapping mode using standard silicon probe.

Results and discussion

Synthesis

For a comparative study, two new homochiral copper 4(5),4′(5′),4″(5″),4‴(5‴)-tetrakis(1-(*p*-tolyl)ethylaminocarbonyl)-phthalocyanines bearing four enantiopure (*S*)-aralkyl moieties, CuPc-(*S*), four enantiopure (*R*)-aralkyl moieties, CuPc-(*R*), and a racemic mixture of (*S*)- and (*R*)-aralkyl moieties, CuPc-(*RS*), were prepared (ESI†, Scheme S1).[9]

IR and MALDI-TOF mass spectra were employed to prove these compound structures. However, ^{1}H-NMR spectrum was not suited to characterising these compounds due to the presence of paramagnetic Cu(II) ion of Pcs. MALDI-TOF MS spectrum revealed that the molecular ion peaks of the CuPc-(*R*), CuPc-(*S*) and CuPc-(*RS*) molecules all show 1221 $[M + H]^+$ (ESI†, Fig. S1). Furthermore, the self-assemblies of CuPc-(*R*), CuPc-(*S*) and CuPc-(*RS*) up to the pentameric state were all clearly detected by this mass spectrometric technique, which revealed a strong interaction between CuPc rings, even in gas phase. These results were similar to those of NiPc.[9] The typical IR peaks (3265 cm^{-1} (ν_{N-H}), 2962, 2922 cm^{-1} (ν_{Ar-C-H}), 2854 cm^{-1} (ν_{C-H}), 1631 cm^{-1} ($\nu_{C=O}$) and 1540 cm^{-1} (ν_{C-N} and δ_{C-H})) due to amide groups of CuPc-(*R*), CuPc-(*S*) and CuPc-(*RS*) were all clearly observed (Fig. S2†).

Self-assembly of CuPc-(*S*) and CuPc-(*R*) in dilute solution

Electronic absorption spectra provide useful information of self-assembling structures, such as face-to-face, edge-to-edge, and herringbone arrangements of π-conjugated molecules.[4b] In particular, non-polar solvents play a crucial role in self-assembling π-conjugated molecules into specific higher order structures.[10]

Visible absorption and CD spectra of CuPc-(*S*) in chloroform ($CHCl_3$) and tetrahydrofuran (THF) are displayed in Fig. 1. Visible spectra of CuPc-(*S*) in THF (λ_{max} = 606 nm) and $CHCl_3$ (λ_{max} = 596 nm) showed a broad, highly

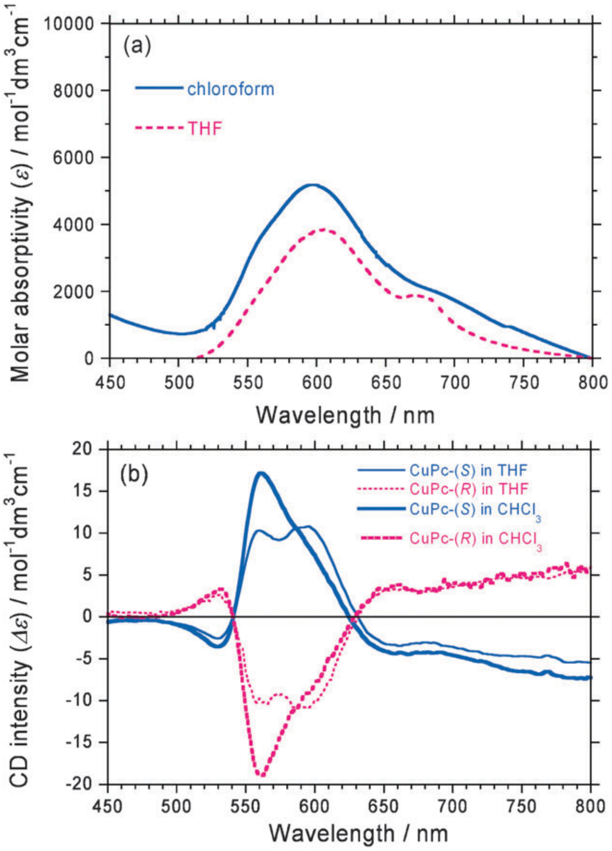

Fig. 1 (a) Visible spectra of CuPc-(*S*) in $CHCl_3$ and THF at 25 °C and (b) CD spectra of CuPc-(*S*) and CuPc-(*R*) in $CHCl_3$ and THF at 25 °C. All concentrations were 5.0×10^{-5} mol L^{-1}.

blue-shifted Q-band. However, CuPc-(*S*) in DMF exhibits λ_{max} at 680 nm which is typical of a monomeric Pc species (Fig. S3, ESI†), possibly, due to the loss of hydrogen bonding.[9]

The aggregation behaviour in THF and $CHCl_3$ is evident. The blue-shifted Q-band absorption originates from the exciton coupling interaction among the regularly aligned transition dipole moments of so-called "H-aggregate", that was already demonstrated by several studies of cofacially arranged Pc self-assembly with the help of peripheral groups, 1-D Pc oligomers and 1-D Pc polymers.[6d–f,9]

The CD spectra of CuPc-(*S*) and CuPc-(*R*) in $CHCl_3$ and THF are given in Fig. 1(b). The CD spectrum of CuPc-(*S*) in $CHCl_3$ shows an intense positive-sign Cotton band at 562 nm. However, CuPc-(*S*) in THF showed two CD signals at 562 nm and 590 nm, which may be due to the different origin of the Q-band transitions. A plausible explanation for this is the coexistence of two types of CuPc supramolecules: the 562 nm-CD band is due to π–π stacks with a high assembling number and the 590 nm-CD band is from π–π stacks with a low assembling number, such as dimer, trimer, and tetramer, and so on, solvated by THF molecules.

For comparison, visible absorption and CD spectra of CuPc-ttb in $CHCl_3$ at 25 °C at three concentrations (0.5×10^{-4}, 1.0×10^{-4}, and 2.0×10^{-4} mol L^{-1}) are shown in Fig. 2. When the concentration increased from 0.5×10^{-4} to 2.0×10^{-4} mol L^{-1}, intensity of the Q-band at 670 nm due to monomeric species markedly decreased. Conversely, the Q-band around 550–700 nm weakened and broadened, possibly, due to the production of certain assembling species. Cotton CD signal at the Q-band region from CuPc-ttb assemblies even at the highest concentration (2.0×10^{-4} mol L^{-1}) cannot be detected. It was concluded that the CuPc-ttb assemblies are not optically active species.

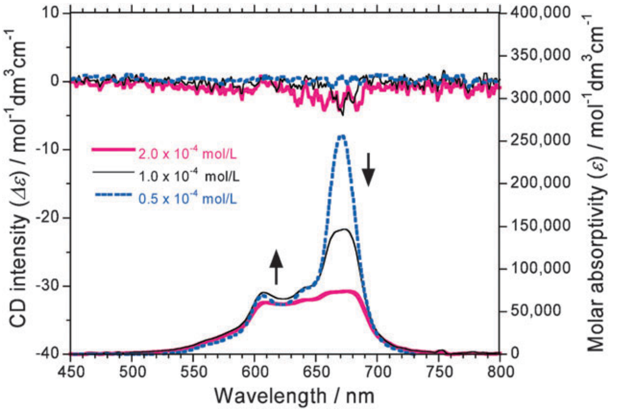

Fig. 2 Visible and CD spectra of CuPc-ttb in $CHCl_3$ at 25 °C with three concentrations, $(0.5–2.0) \times 10^{-4}$ mol L^{-1}. For measurement at 2.0×10^{-4} mol L^{-1}, a cuvette with 1 mm path length was used.

On the other hand, when CuPc-(*S*) molecule was dissolved in DMF, any Cotton CD signals were not detected, possibly, due to the loss of intermolecular hydrogen bonding (Fig. S3, ESI†). Any Cotton CD signals from CuPc-(*RS*) in $CHCl_3$ (Fig. S4†) were not detected though λ_{max} appeared at 590 nm, suggesting the production of π–π stacked assemblies. The CD spectra of CuPc-(*R*) gave negative-sign Cotton signals due to the blue-shifted Q-band at 550–600 nm in $CHCl_3$ and THF (Fig. 1(b) and Fig. S5, ESI†).

The chiroptical properties of CuPc-(*S*) and CuPc-(*R*) supramolecules in $CHCl_3$, which is a measure of degree of helicity, can be semi-quantitatively evaluated by the dimensionless Kuhn's dissymmetry ratio, defined as $g_{abs} = \Delta\varepsilon/\varepsilon$, where $\Delta\varepsilon$ is molar ellipticity and ε is molar absorptivity. The values of g_{abs} at 562 nm, which is an extremum of Cotton CD Q-band, were evaluated to be $+8.53 \times 10^{-3}$ for CuPc-(*S*) and -8.62×10^{-3} for CuPc-(*R*), respectively. The almost identical absolute g_{abs} values of CuPc-(*S*) and CuPc-(*R*) indicate that the helicity of CuPc-(*S*) and CuPc-(*R*) supramolecules is the opposite. These led to the idea that the optically active supramolecular CuPc structures are almost in a mirror image relationship, in which helicity was induced by the peripheral group homochirality.

The marked difference in visible spectral characteristics of CuPc-(*S*) and NiPc-(*S*) in $CHCl_3$ is evident (Fig. 3). The value of λ_{max} (596 nm) of CuPc-(*S*) in a poor solvent $CHCl_3$ was red-shifted by 35 nm when compared to that (561 nm) of NiPc-(*S*), though they carry commonly four enantiopure groups at their peripheral positions. Self-assembling ability of CuPc-(*S*) is a little weaker than that of NiPc-(*S*).

Visible absorption spectra of CuPc-(*S*) and NiPc-(*S*) dissolved in 1,1,2,2-tetrachloroethane (a poor solvent) at several temperatures are displayed in Fig. 4. From Fig. 4(a),

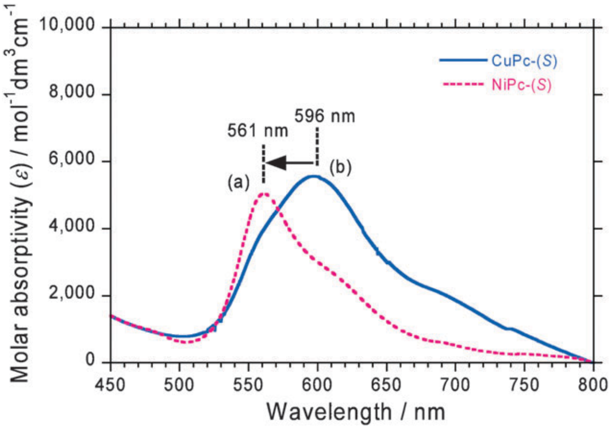

Fig. 3 Visible spectra of CuPc-(*S*) and NiPc-(*S*) in $CHCl_3$ (5.0×10^{-5} mol L^{-1}). NiPc-(*S*) prepared previously was used.[9]

when solution temperature increased from −5 to 110 °C, the intensities of the two Q-bands at 682 nm and 615 nm, which are due to monomeric and weakly assembled species (dimer, trimer and so on), respectively, markedly increased, while the broad Q-band around 600 nm due to highly assembled species progressively decreased.

On the other hand, from Fig. 4(b), NiPc-(*S*) self-assembly possesses a high thermal stability even at 110 °C. Also, the λ_{max} value (555 nm) of NiPc-(*S*) is greatly blue-shifted by 41 nm, compared to that of CuPc-(*S*), suggesting the high assembling number of NiPc-(*S*). As solution temperature increased from −5 °C to 110 °C, the intensities of the 680 nm and 615 nm Q-bands slightly increased while the intensity of the 600 nm Q-band showed a very weak temperature dependency. These observations led to an idea that the self-assembling ability of CuPc-(*S*) is more sensitive to temperature than that of NiPc-(*S*), as is shown in Fig. 4. Subtle difference is only that Cu(II) is paramagnetic and Ni(II) is diamagnetic, in which both are weakly coordinated in chloroform and 1,1,2,2-tetrachloroethane solvents.

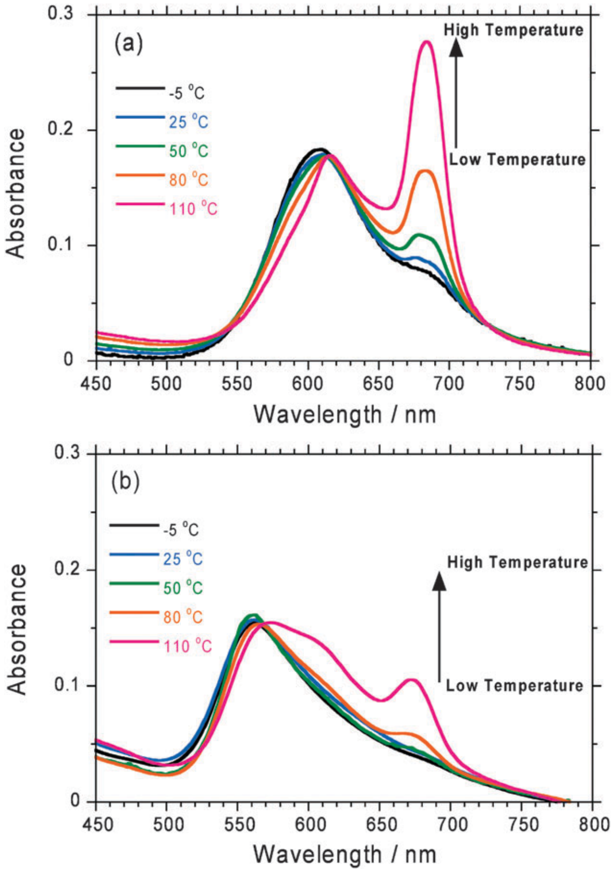

Fig. 4 Temperature dependence of visible absorption spectra of (a) CuPc-(*S*) and (b) NiPc-(*S*) in 1,1,2,2-tetrachloroethane (1.0×10^{-5} mol L^{-1}).

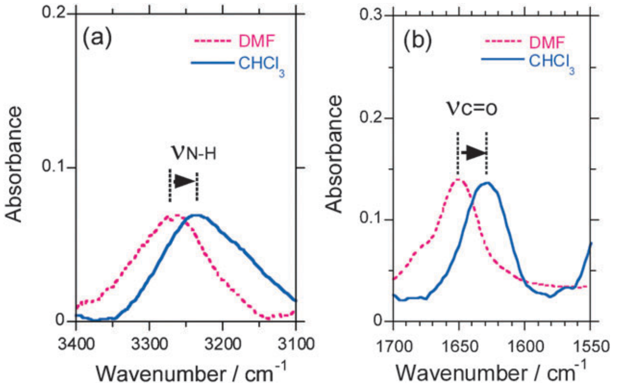

Fig. 5 IR spectra of CuPc-(*S*) film on CaF_2 at 25 °C casting from its $CHCl_3$ and DMF solutions.

Solvent dependency of the self-assembling ability of CuPc-(*S*) is evident from FT-IR measurement (Fig. 5). When solutions of CuPc-(*S*) dissolved in DMF and chloroform were cast on CaF_2 substrate, IR vibrations due to secondary amide group in the ν_{N-H} and $\nu_{C=O}$ regions were much different. The ν_{N-H} vibration from chloroform solution appeared at 3235 cm^{-1}, red-shifted by 30 cm^{-1}, compared to that from DMF solution, 3265 cm^{-1} (Fig. 5a). Similarly, the $\nu_{C=O}$ vibration cast from chloroform solution appeared at 1630 cm^{-1} which was red-shifted by 20 cm^{-1}, compared to that from DMF solution, 1650 cm^{-1} (Fig. 5b). These red-shifting behavior of secondary amide groups are due to the loss of intermolecular hydrogen bonding of 1-(*p*-tolyl)ethylamino-carbonyl groups at their peripheral positions.

Solvent DMF molecules are assumed to weaken the intermolecular hydrogen bonding interactions of CuPc-(*S*) and, possibly, of CuPc-(*R*) and CuPc-(*RS*) supramolecular assemblies. The weakening of intermolecular hydrogen bonding interaction is responsible for the disappearance of CD of CuPc-(*S*) and CuPc-(*R*) in DMF. The effective intermolecular hydrogen bonding interaction is dominantly responsible for the appearance of Cotton CD signals of CuPc-(*S*) and CuPc-(*R*) when they were dissolved in poor solvents including $CHCl_3$, THF and 1,1,2,2-tetrachloroethane.

Self-assembly of CuPc-(*S*) and CuPc-(*R*) in the solid state

Controlled transfer of helical self-assembly from dilute solution to the solid surface still remains a challenge while keeping the integrity of preferential handedness. This is because the weak noncovalent interactions involved in the helical supramolecules in the solution are difficult to be kept on the solid surface due to strong interactions between the supramolecules and the surface.[11]

From wide-angle X-ray diffraction (WAXD) measurement (Fig. 6), CuPc-(*S*) showed two major diffraction peaks at 2*θ* ~4.09° and ~26.84°, corresponding to *d*-spacings of ~21.61 Å and ~3.32 Å, respectively, whereas NiPc-(*S*) powders showed two major diffraction peaks at 2*θ* ~3.90° and ~27.02°, corresponding to *d*-spacings of ~22.65 Å and ~3.45 Å, respectively.[9] The Pc ring separation in the CuPc assembly may be ~3.32 Å which corresponds to van der Waals thickness of aromatic ring. This led to an idea that CuPc-(*S*) adopts face-to-face π–π stacks, possibly, 1-D like structure, which is similar to NiPc-(*S*) and NiPc-(*R*) stacking structures reported previously.[9]

The CD and visible spectra in thin solid films of CuPc-(*R*), CuPc-(*S*) and CuPc(*RS*) are given in Fig. 7. Compared to CD spectra in $CHCl_3$, solid-state CD spectra of CuPc-(*R*) and CuPc-(*S*) became broad and the CD extremum red-shifted by ~50 nm, which may be due to intercolumnar interaction between 1-D Pc stacks. In these thin films, all the λ_{max} values of the Q-band were found at 595 nm, which is similar to those in $CHCl_3$. Although the CD spectra of CuPc-(*R*) and CuPc-(*S*) have a nearly mirror image relationship, any detectable CD signals of CuPc-(*RS*) cannot be seen. This implies that optically inactive PcCu-(*RS*) supramolecules in the solid state may exist as a conglomerate with the opposite helical sense. The reason may be that the CuPc-(*S*) and CuPc-(*R*) are able to self-organise into 1-D architecture with left-handed and right-handed helicity in solution, respectively.

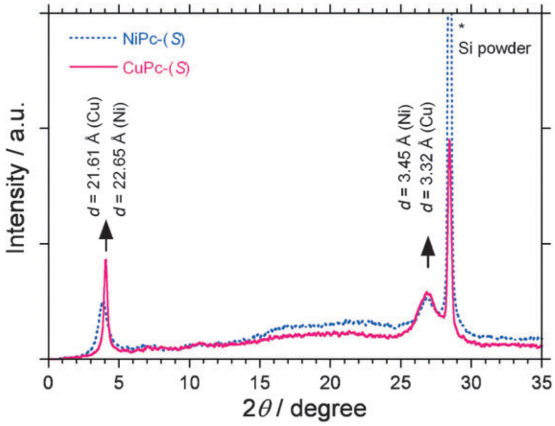

Fig. 6 Wide-angle X-ray diffraction patterns of CuPc-(*S*) and NiPc-(*S*) powders.

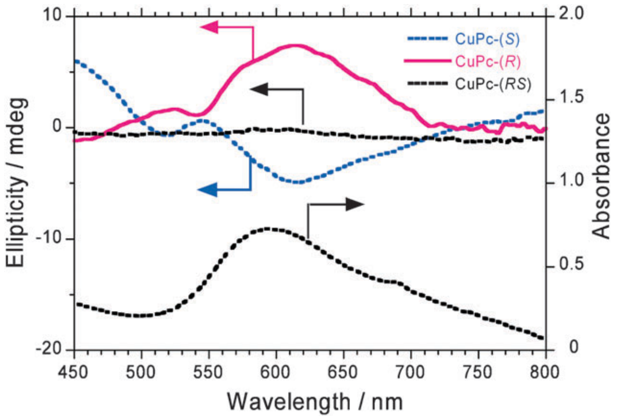

Fig. 7 CD spectra of CuPc-(*S*), CuPc-(*R*) and CuPc-(*RS*) films on quartz and visible absorption spectrum of CuPc-(*S*), CuPc-(*R*) or CuPc-(*RS*) film on quartz.

Note that Cotton CD spectra of CuPc-(*R*) and CuPc-(*S*) in their thin films are absolutely opposite compared with those of CuPc-(*R*) and CuPc-(*S*) in $CHCl_3$ solution. Ramaiah *et al.* reported a similar phenomena for chiral supramolecular assembly of squaraine dye.[10a] The reason for this remains unclear.

AFM imaging of CuPc-(*S*), CuPc-(*R*), Cu-Pc(*RS*) and CuPc-ttb assemblies on mica

High-resolution AFM imaging technique with the tapping mode provides the morphology of molecular assemblies on solid surface. AFM images of CuPc-(*S*) and CuPc-(*R*) assemblies on mica surface are depicted in Fig. 8(A) and (B). For comparison, AFM images of CuPc-(*RS*) and CuPc-ttb assemblies on mica surface are displayed in Fig. 8(C) and (D), respectively. The specimens of CuPc-(*S*), CuPc-(*R*) and CuPc-(*RS*) for AFM study were prepared by casting their $CHCl_3$ solution (1×10^{-4} mol L^{-1}) on freshly cleaved mica substrates, respectively, by controlling the concentration. The specimen of CuPc-ttb was prepared by casting its $CHCl_3$ solution (2×10^{-5} M) on mica substrate.

From Fig. 8(A)–(C), it is evident that CuPc-(*S*), CuPc-(*R*) and CuPc-(*RS*) adopt highly entangled networks composed of many fibers regardless of peripheral chirality. From the section analysis, the height of these fibers of CuPc-(*S*) and CuPc-(*R*) on the mica ranged from 1.4 to 2.0 nm (Fig. S8, ESI†), which may correspond to the height of a single Pc molecule itself. The shape of fibers, however, is not highly extended rod-like

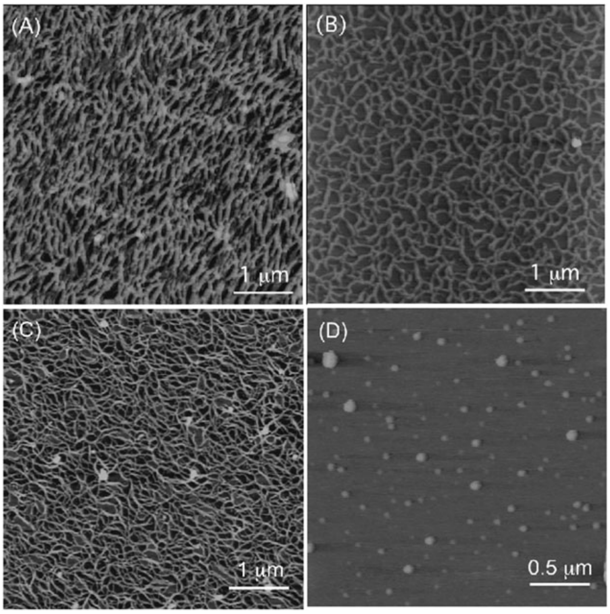

Fig. 8 AFM images on mica cast from dilute $CHCl_3$ solutions of (A) CuPc-(*S*) (1×10^{-4} mol L^{-1}), (B) CuPc-(*R*) (1×10^{-4} mol L^{-1}), (C) CuPc-(*RS*) (1×10^{-4} mol L^{-1}) and (D) CuPc-ttb (2×10^{-5} mol L^{-1}).

structures which were frequently seen in NiPc-(*R*) assemblies on mica as reported previously (Fig. S9, ESI†).[9] CuPc-(*S*), CuPc-(*R*) and CuPc-(*RS*) favor worm-like structures on mica. In an analogy with chain-like polymers, these CuPc supramolecular polymers have a shorter persistence length and the NiPc supramolecular polymers have a longer persistence length though the CuPcs and NiPc have the same chiral peripheral groups. Contrarily, CuPc-ttb assemblies showed dot-like structures due to a very weak π–π stacking ability of *tert*-butyl groups only.

When specimens on mica cast from different concentrations of CuPc-(*R*) were employed, the networks composed of many worm-like structures turned to several isolated worm-like structures including circle-like and semi-circle-like structures (Fig. 9). As demonstrated previously, σ-conjugated polysilane with semi-flexible helical main chain[12] and π-conjugated polyfluorenes with semi-flexible main chain[13] are possible to form similar circle-like and semi-circle-like structures onto mica surface by casting its dilute solution under controlled conditions.

Compared to the Ni(II)Pcs, the origin of the structural adaptability of Cu(II)Pcs remains unclear. There exists subtle difference in ionic radii between tetra-coordinate, square-type Cu(II) (0.057 nm) and Ni(II) (0.049 nm) ions.[14] The major difference between Cu(II) and Ni(II) is their paramagnetic and diamagnetic properties, respectively. Paramagnetic Cu(II) ions are assumed to be responsible for the structural adaptability of the Cu(II)Pcs.

The AFM results combined with WAXD and CD/visible spectroscopic studies led to an idea that CuPc-(*S*), CuPc-(*R*) and CuPc-(*RS*) can form supramolecular polymers and circle-like and semi-circle-like structures on mica, possibly, in fluid solution and in the solid. The peripheral homochirality might contribute to the preferential twist sense of assemblies which give the optically active Q-band.

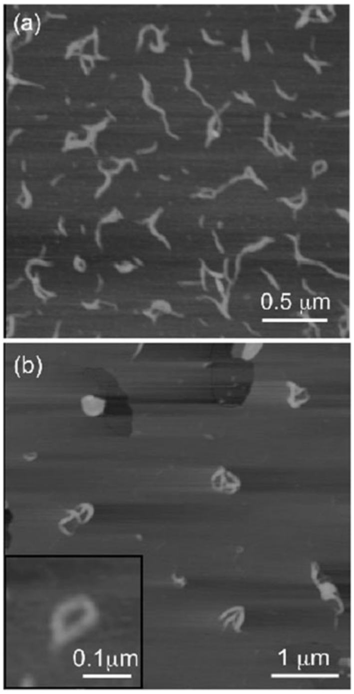

Fig. 9 AFM images of CuPc-(*R*) on mica cast from $CHCl_3$ solutions of (a) 5 × 10^{-5} mol L^{-1} and (b) 1 × 10^{-5} mol L^{-1}.

Magnetic properties of CuPc-(*S*) and CuPc-(*R*) assemblies

Cu(II) has paramagnetic ion due to d^9 electron system. CuPc-(*S*) assemblies may have a potential of paramagneticity due to a large number of coupled paramagnetic centers. The design and preparation of molecular and supramolecular materials due to the intrinsic low symmetry in favor of 1-D arrangements is recently been documented.[15] Unsubstituted Cu(II)Pc (1.75 BM) crystal did not undergo magnetic ordering transition down to 1.8 K.[16] Substituted CuPc with crownether moiety in the presence of Na as counter ion has shown to exhibit paramagnetic spin coupling due to dimerisation by electron paramagnetic resonance measurement (EPR) study.[17] Several workers reported magnetic behaviours of Pc compounds containing metal ions.[17] Recently, El Fallah and coworkers reported preliminarily ferromagnetic behavior of amino-pyridine Cu(II) complex with 2-D sheet structure below 50 K.[19]

As CuPc-(*S*) and CuPc-(*R*) assemblies are supramolecular polymers composed of number of paramagnetic Cu(II) ions, we anticipated the paramagnetic, ferromagnetic and anti-ferromagnetic behavior of these supramolecules.

A preliminary measurement of magnetic properties of CuPc-(*S*) film cast on mica and Si substrate using a vibrating sample magnetometer (Riken Denshi, BHV-525RSCM) was employed in attempting detection of magnetic ordering from the CuPc samples at various temperatures (20 K, 50 K, 100 K, 150 K and room temperature). However, no conclusive evidence of such magnetic ordering was yielded (Fig. S6, ESI†). However, a preliminary EPR measurement (JEOL, JES-FA100N) of CuPc-(*S*) (1 × 10^{-4} mol L^{-1}) in chloroform at room temperature exhibited magnetic coupling due to Cu(II) (Fig. S7†), which is similar to supramolecular dimer of the CuPc with crownethers.[17]

Magnetic force microscopy (MFM) technique allows to study the local magnetic field gradient of terbium(III) Pc dimer on diamagnetic HOPG surface.[18] To test the possibility of magnetic ordering of CuPc-(*R*) supramolecular fibers onto mica, which was prepared by casting from 1 × 10^{-4} mol L^{-1} chloroform solution, MFM experiments were employed. A preliminary MFM imaging was conducted by a Veeco NanoScope IIIa with an MFM mode (model MESP: Sb-doped Si cantilever coated with Co/Cr, lift scan height of 20 nm) (Fig. S10, ESI†).

The specimen was shown to have worm-like images by AFM observation prior to the MFM measurement. Several worm-like images due to the PcCu-(*R*) origin on mica exhibited less magnetic contrast because they appeared to be visualised weakly at room temperature. The question opens whether the origin of worm-like magnetic image comes from certain inherent magnetic ordering or 1-D paramagnetism, which is a highly fluctuating magnetic ordering induced by an external Co/Cr-tip cantilever. There exists no conclusive evidence of an intense magnetic ordering because PcCu-(*R*) supramolecular polymers do not provide a proper magnetic contrast. Further careful design and synthesis of four-fold molecular symmetry

MPc supramolecular polymer systems arranged to two- and three-dimensional lattices may give an answer to this question.

Energy diagram of CuPc-(*S*) and CuPc-(*R*) assemblies

Unpolarised electronic and CD spectra of CuPc-(*S*) and CuPc-(*R*) supramolecular assemblies in chloroform are re-plotted as a function of photon energy in electron volt. The original data were taken from Fig. 1 and Fig. 2 and Fig. S5 (ESI†). It is evident that CuPc-(*S*) and CuPc-(*R*) have two extrema at 2.22 eV and 1.54 eV with opposite signs. Although the values of $|g_{\mathrm{abs}}|$ at 2.22 eV (562 nm) and at 1.54 eV (805 nm) attain $\sim 8.6 \times 10^{-3}$ and $\sim 3 \times 10^{-2}$, respectively.

According to the point dipole exciton approximation developed by Kasha *et al.*,[20] the energy shift (ΔE) between the exciton band for 1D infinite chain stack of dyes and its monomer, when the end effects are neglected, is given as follows:

$$\begin{aligned}\Delta E &= E_{\mathrm{a}} - E_{\mathrm{m}}\\ &= 2 \times \left|\left(\frac{N-1}{N}\right)\left(\frac{M^2}{r^3}\right)(\cos\alpha - 3\cos^2\beta)\right|\end{aligned} \qquad (1)$$

where E_{a} and E_{m} are the respective assemblies and monomer transition energies, N the association number of the stack, M the transition dipole strength, r the closest ring spacing between the transition moments, α the torsion angle between the moments, and β the tilt angle. From the selection rule, the theory has predicted that when $0° < \beta < 54.7°$ the electrically allowed transition of assemblies red-shifts, and when $54.7° < \beta < 90°$, the electrically allowed transition will be blue-shifted. Conversely, when $0° < \beta < 54.7°$ the electrically forbidden transition of the assemblies will be blue-shifted and when $54.7° < \beta < 90°$, the electrically forbidden transition will be red-shifted.

The value of M is given as:

$$M = \frac{3\hbar e^2 f}{8\pi^2 m_{\mathrm{e}} c g_n E_{\mathrm{m}}}\ \mathrm{erg\,cm^3} \qquad (2)$$

where $\hbar$ is the Planck constant, e the electronic charge, m_{e} the electron mass, c the velocity of light in vacuum, g_n the degeneracy of the excited state, and f the oscillator strength.

The value of f is calculated by

$$f = 4.32 \times 10^{-9} \int_{\nu_1}^{\nu_2} \varepsilon d\nu\ \mathrm{erg\,cm^3} \qquad (3)$$

where ε is the molar absorptivity in $\mathrm{M^{-1}\,cm^{-1}}$ and ν_1 and ν_2 are the initial and final frequencies of the monomer absorption band in $\mathrm{cm^{-1}}$. Eqn (1) simply predicts that the maximum value of ΔE may be further changed, if 1-D Pc stacks with a high assembling number were able to adopt an ideal eclipsed form with $\alpha = 0°$ and $\beta = 90°$, assuming that the 1-D Pc supramolecular polymers in solution and in the powder may adopt $\alpha = 45°$ (full staggered form), $\alpha = 22.5°$ (partly staggered form), or $\beta \neq 90°$ (tilted form). The ΔE in the case of $\alpha = 0°$ is possible to further increase by 1.4 times when compared to the ΔE in the case of $\alpha = 45°$, leading to the maximum ΔE of $\sim 2500\ \mathrm{cm^{-1}}$. To semi-empirically evaluate the assembling number in the 1-D Pc stacks, eqn (1) reduces as follows:

$$N = \frac{\Delta E(N \to \infty)}{\Delta E(N \to \infty) - \Delta E(N)} \qquad (4)$$

where $\Delta E(N)$ is the exciton shift for the 1-D Pc stacks with assembling number of N and $\Delta E(N \to \infty)$ the exciton shift for the infinite Q1D Pc stacks. Eqn (2) indicates that the exciton shift ΔE value of the dimer is just half that of the 1-D infinite chain. If the transition energies in both the dimer and monomer or in both the infinite stacks and monomer are obtained experimentally, the assembling number could be evaluated.

If CuPc-(*S*) and CuPc-(*R*) assemblies in $\mathrm{CHCl_3}$ solution are assumed to adopt Q1D Pc stacks with a high association number, the exciton shift ΔE from the allowed Q-band transitions between the assemblies (2.22 eV or 562 nm) and monomeric species (1.82 eV or 680 nm) of CuPc is estimated to ~ 0.40 eV ($\sim 3230\ \mathrm{cm^{-1}}$). In a similar way, the exciton shift ΔE from the forbidden Q-band transition (1.54 eV or 805 nm) of the assemblies and the allowed Q-band transition of monomeric species is estimated to ~ 0.28 eV ($\sim 2260\ \mathrm{cm^{-1}}$).

If the CuPc-(*S*) and CuPc-(*R*) adopt helical assemblies, the allowed and forbidden exciton bands may exhibit two Cotton CD signals. From the sum rule,[21] two Cotton CD signals are the opposite sign with an equal rotatory strength, as can be seen as apparent bisignate Cotton CD bands in Fig. 10.

From the above consideration, an energy diagram of CuPc-(*S*) supramolecular assembly with a preferential helical sense is proposed in Fig. 11. The negative-sign, Cotton Q-band at 1.54 eV may be an electrically forbidden, magnetically allowed transition from the top of the highest occupied valence band (HOVB) to the bottom of the lowest unoccupied conduction band (LUCB), while the positive-sign, Cotton Q-band at 2.22 eV is an electrically allowed, magnetically allowed transition from the bottom of HOVB to the top of LUCB.

From the viewpoint of supramolecular chemistry, π–π stacking nature may be inherent of large macrocyclic Pc rings. Slippery nature is, however, possible to fix with the help of hydrogen-bonding interactions between secondary amide groups. Twist sense is controlled by point chirality of the homochiral peripheral groups. The present results of CuPc-(*R*)

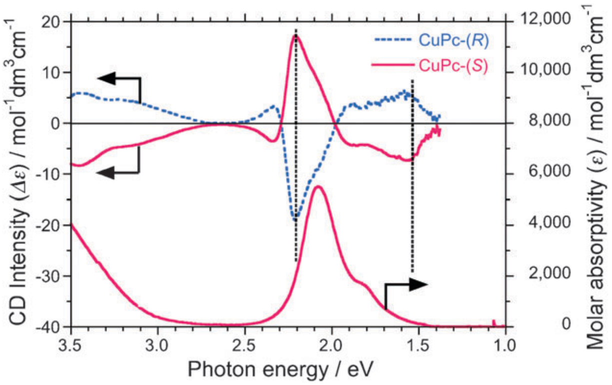

Fig. 10 A broad range unpolarised electronic and CD spectra of CuPc-(*S*) and CuPc-(*R*) supramolecular assemblies in $\mathrm{CHCl_3}$. The original data were taken from Fig. 1 and Fig. 2 and Fig. S5 (ESI†).

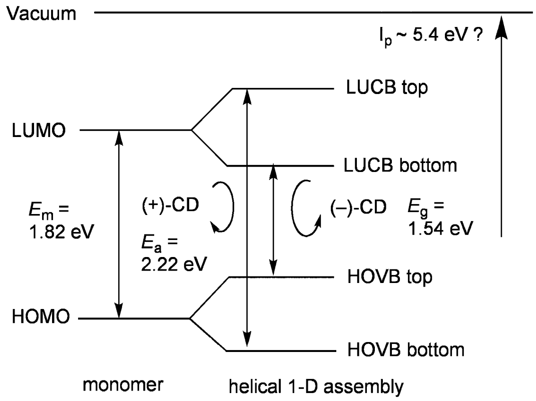

Fig. 11 A proposed energy diagram of CuPc-(*S*) supramolecular assembly with a preferential helix sense.

and CuPc-(*S*) are based on the design by learning the nature's elegant bottom-up programming, though a left–right preference in biological chirality remains an unsolved issue. The origin of difference between Cu(II) and Ni(II) in the Pc system is also unclear.

Conclusion

Inspired by the nature's bottom-up programming with homochiral building blocks, the self-assembling features of CuPc-(*S*), CuPc-(*R*) and CuPc-(*RS*) were studied by means of visible, CD and IR spectroscopic study along with WAXD and scanning probe microscope measurements. AFM study revealed that the supramolecular polymers made of CuPc-(*S*), CuPc-(*R*) and CuPc-(*RS*) are able to form worm-like fibers onto mica surface. The quadruple hydrogen bonding between the secondary amides of neighboring CuPc molecules, along with Pcπ–Pcπ stacking and homochiral interactions, were responsible for production of optically active CuPc assemblies and supramolecular polymers.

Acknowledgements

Wei Zhang is grateful for the financial support from the JSPS fellowship (FY2009–FY2010). The work was partly supported from Grant-in-Aid for Scientific Research (16202017, FY2004-FY2007 and 22350052, FY2010–FY2013) and the Sekisui Chemical Grant Program for Research on Manufacturing Based on Learning from Nature (FY2010). We thank Prof. Kotohiro Nomura and Dr Yoko Nakano for fruitful discussion and valuable comments. We thank Prof. Nobuyoshi Hosoito and Dr Kenji Kodama for a preliminary measurement of magnetic properties of CuPc-(*S*) film cast on mica and Si using a vibrating sample magnetometer in attempting detection of magnetic ordering of the CuPc samples.

References

1 (*a*) D. R. Eyre, *Science*, 1980, **207**, 1315; (*b*) H. Engelkamp, S. Middelbeek and R. J. M. Nolte, *Science*, 1999, **284**, 785; (*c*) L. Brunsveld, B. J. B. Folmer, E. W. Meijer and R. P. Sijbesma, *Chem. Rev.*, 2001, **101**, 4071; (*d*) J. P. Hill, W. Jin, A. Kosaka, T. Fukushima, H. Ichihara, T. Shimomura, K. Ito, T. Hashizume, N. Ishii and T. Aida, *Science*, 2004, **304**, 1481.

2 (*a*) D. N. Reinhoudt and M. Crego-Calama, *Science*, 2002, **295**, 2403; (*b*) G. M. Whitesides, J. P. Mathias and C. T. Seto, *Science*, 1991, **254**, 1312; (*c*) F. Gulik-Krzywicki, C. Fouquey and J.-M. Lehn, *Proc. Natl. Acad. Sci. U. S. A.*, 1993, **90**, 163; (*d*) S. Mihai, A. Cazacu, C. Arnal-Herault, G. Nasr, A. Meffre, A. van der Lee and M. Barboiu, *New J. Chem.*, 2009, **33**, 2335; (*e*) Y. Nakano, Y. Liu and M. Fujiki, *Polym. Chem.*, 2010, **1**, 460; (*f*) O. V. Kulikov, N. P. Rath, D. Zhou, I. A. Carasel and G. W. Gokel, *New J. Chem.*, 2009, **33**, 1563; (*g*) M. Fujiki, *Chem. Rec.*, 2009, **9**, 271.

3 (*a*) D. Y. Yan, Y. F. Zhou and J. Hou, *Science*, 2004, **303**, 65; (*b*) P.-Z. Li, X.-M. Lu, B. Liu, S. Wang and X.-J. Wang, *Inorg. Chem.*, 2007, **46**, 5823; (*c*) K. S. Min and M. P. Suh, *Eur. J. Inorg. Chem.*, 2001, 449; (*d*) M. Tiitu, N. Volk, M. Torkkeli, R. Serimaa, G. Brinke and O. Ikkala, *Macromolecules*, 2004, **37**, 7364; (*e*) Y. Liu, Z. Fan, H.-Y. Zhang and C.-H. Diao, *Org. Lett.*, 2003, **5**, 251; (*f*) O. Ikkala and G. Brinke, *Science*, 2002, **295**, 2407; (*g*) X.-L. Tang, W.-H. Wang, W. Dou, J. Jiang, W.-S. Liu, W.-W. Qin, G.-L. Zhang, H.-R. Zhang, K.-B. Yu and L.-M. Zheng, *Angew. Chem., Int. Ed.*, 2009, **48**, 3499; (*h*) T. Nakano, *Polym. J. (Tokyo)*, 2010, **42**, 103; (*i*) T. Nakano and T. Yade, *J. Am. Chem. Soc.*, 2003, **125**, 15474.

4 (*a*) C.-Y. Liu, H.-L. Pan, M. A. Fox and A. J. Bard, *Science*, 1993, **261**, 897; (*b*) C. Y. Liu, H. L. Pan, M. A. Fox and A. J. Bard, *Chem. Mater.*, 1997, **9**, 1422; (*c*) L. Schmidt-Mende, A. Fechtenkotter, K. Mullen, E. Moons, R. H. Friend and J. D. MacKrnzie, *Science*, 2001, **293**, 1119; (*d*) M. Kimura, H. Ueki, K. Ohta, H. Shirai and N. Kobayashi, *Langmuir*, 2006, **22**, 5051; (*e*) M. Kimura, T. Kuroda, K. Ohta, K. Hanabusa, H. Shirai and N. Kobayashi, *Langmuir*, 2003, **19**, 4825; (*f*) B. A. Gregg, M. A. Fox and A. J. Bard, *J. Phys. Chem.*, 1989, **93**, 4227; (*g*) M. Hanack, D. Dini, M. Barthei and S. Vagin, *Chem. Rec.*, 2002, **2**, 129; (*h*) T. J. Marks, *Angew. Chem., Int. Ed. Engl.*, 1990, **29**, 857; (*i*) J. Simon and C. Sirlin, *Pure Appl. Chem.*, 1989, **61**, 1625; (*j*) H. Iino, J. I. Hanna, R. J. Bushby, B. Movaghar, B. J. Whitaker and M. J. Cook, *Appl. Phys. Lett.*, 2005, **87**, 132102; (*k*) R. S. Nohr, P. M. Kuznesof, K. J. Wynne, M. E. Kenney and P. G. Siebenman, *J. Am. Chem. Soc.*, 1981, **103**, 4371; (*l*) K. Ohta, K. Hatsusaka, M. Sugibayashi, M. Ariyoshi, K. Ban, F. Maeda, R. Naito, K. Nishizawa, A. M. van de Craats and J. M. Warman, *Mol. Cryst. Liq. Cryst.*, 2003, **397**, 325; (*m*) F. Nekelson, H. Monobe and Y. Shimizu, *Chem. Commun.*, 2006, 3874.

5 (*a*) J. J. W. M. Rosink, M. A. Blauw, L. J. Geerligs, E. van der Drift, B. A. C. Rousseeuw and S. Radelaer, *Langmuir*, 2000, **16**, 4547; (*b*) Q. Xu, H. Ma, H. Yip and A. K.-Y. Jen, *Nanotechnology*, 2008, **19**, 135605; (*c*) K. Okamoto, P. Chithra, G. J. Richards, J. P. Hill and K. Ariga, *Int. J. Mol. Sci.*, 2009, **10**, 1950; (*d*) N. R. Armstrong, W. N. Wang, D. M. Alloway, D. Placencia, E. Ratcliff and M. Brumbach, *Macromol. Rapid Commun.*, 2009, **30**, 717.

6 (*a*) T. Inabe and H. Tajima, *Chem. Rev.*, 2004, **104**, 5503; (*b*) M. J. Stillman and T. Nyokong, in *Phthalocyanines: Properties and Applications*, ed. C. C. Leznoff and A. B. P. Lever, VCH, New York, 1989; (*c*) M. Fujiki, H. Tabei and K. Isa, *J. Am. Chem. Soc.*, 1986, **108**, 1532; (*d*) M. Fujiki and H. Tabei, *J. Phys. Chem.*, 1988, **92**, 1281; (*e*) M. Fujiki, H. Tabei and T. Kurihara, *Langmuir*, 1988, **4**, 1123; (*f*) M. Fujiki and H. Tabei, *Langmuir*, 1988, **4**, 320; (*g*) M. Hanack and M. Lang, *Adv. Mater.*, 1994, **6**, 819; (*h*) Z. Ji, M. Liu, L. Shang, W. Hu, G. Liu, X. Liu and H. Wang, *J. Mater. Chem.*, 2009, **19**, 5507; (*i*) I. Yilmaz, *New J. Chem.*, 2008, **32**, 37.

7 (*a*) N. Kobayashi, H. Lam, W. A. Nevin, P. Janda, C. C. Leznoff, T. Koyama, A. Monden and H. Shirai, *J. Am. Chem. Soc.*, 1994, **116**, 879; (*b*) M. Inagawa, H. Yoshikawa, T. Yokoyama and K. Awaga, *Chem. Commun.*, 2009, 3389; (*c*) K. Ozawa and K. Ishii, *Phys. Chem. Chem. Phys.*, 2009, **11**, 1019; (*d*) P. Chen, X. Ma and M. Liu, *Macromolecules*, 2007, **40**, 4780; (*e*) D. Neher, *Adv. Mater.*, 1995, **7**, 691; (*f*) M. Idowu, J. Y. Chen and T. Nyokong, *New J. Chem.*, 2008, **32**, 290; (*g*) N. Kobayashi, R. Higashi, B. C. Titeca, F. Lamote and A. Ceulemans, *J. Am. Chem. Soc.*, 1999, **121**, 12018.

8 (*a*) H. Engelkamp, C. F. V. Nostrum, J. S. Picken and R. J. M. Nolte, *Chem. Commun.*, 1998, 979; (*b*) C. F. Van nostrum, A. W. Bosman, G. H. Gelinck, P. G. Schouten, J. M. Warman, A.

P. M. Kentgens, M. A. C. Devillers, A. Meijerink, S. J. Picken, U. Sohling, A. J. Schouten and R. J. M. Nolte, *Chem.–Eur. J.*, 1995, **1**, 171.

9 R. Rai, A. Saxena, A. Ohira and M. Fujiki, *Langmuir*, 2005, **21**, 3957.

10 (*a*) K. Jyothish, M. Hariharan and D. Ramaiah, *Chem.–Eur. J.*, 2007, **13**, 5944; (*b*) S. Jiang, L. Zhang and M. Liu, *Chem. Commun.*, 2009, 6252; (*c*) D. Monti, M. Venanzi, G. Mancini, C. D. Natale and R. Paolesse, *Chem. Commun.*, 2005, 2471; (*d*) M. A. Mateos-Timoneda, M. Crego-Calama and D. N. Reinhoudt, *Chem. Soc. Rev.*, 2004, **33**, 363; (*e*) Y. Li, T. Wang and M. Liu, *Soft Matter*, 2007, **3**, 1312; (*f*) L. Ma and W. Lin, *J. Am. Chem. Soc.*, 2008, **130**, 13834; (*g*) Y. Inoue, H. Ikeda, M. Kaneda, T. Sumimura, S. R. L. Everitt and T. Wada, *J. Am. Chem. Soc.*, 2000, **122**, 406; (*h*) R. A. van Delden, N. P. M. Huck, J. J. Piet, J. M. Warman, S. C. J. Meskers, H. P. J. M. Dekkers and B. L. Feringa, *J. Am. Chem. Soc.*, 2003, **125**, 15659; (*i*) S. Sakurai, K. Okoshi, J. Kumaki and E. Yashima, *J. Am. Chem. Soc.*, 2006, **128**, 5650.

11 (*a*) P. Jonkheijm, F. J. M. Hoeben, R. Kleppinger, J. van Herrikhuyzen, A. P. H. J. Schenning and E. W. Meijer, *J. Am. Chem. Soc.*, 2003, **125**, 15941; (*b*) H. Schonherr, V. Paraschiv, S. Zapotoczny, M. Crego-Calama, P. Timmerman, C. W. Frank, G. J. Vancso and D. N. Reinhoudt, *Proc. Natl. Acad. Sci. U. S. A.*, 2002, **99**, 5024; (*c*) M. Naito and M. Fujiki, *Soft Matter*, 2008, **4**, 211.

12 A. Ohira, S.-Y. Kim, M. Fujiki, Y. Kawakami, M. Naito, G. Kwak and A. Saxena, *Chem. Commun.*, 2006, 2705.

13 Y. Liu, T. Murao, Y. Nakano, M. Naito and M. Fujiki, *Soft Matter*, 2008, **4**, 2396.

14 R. D. Shannon, *Acta Crystallogr., Sect. A: Cryst. Phys., Diffr., Theor. Gen. Crystallogr.*, 1976, **32**, 751.

15 D. Gatteschi and R. Sessoli, *Angew. Chem., Int. Ed.*, 2003, **42**, 268.

16 R. Havemann, W. Haberditzl and K. H. Mader, *Z. Phys. Chem. (Munich)*, 1962, **218**, 71.

17 N. Kobayashi and A. B. P. Lever, *J. Am. Chem. Soc.*, 1987, **109**, 7433.

18 J. Gómez-Segura, I. Diez-Perez, N. Ishikawa, M. Nakano, J. Veciana and D. Ruiz-Molina, *Chem. Commun.*, 2006, 2866.

19 A. Majumder, C. R. Choudhury, S. Mitra, G. M. Rosair, M. S. El Fallah and J. Ribas, *Chem. Commun.*, 2005, 2158.

20 (*a*) M. Kasha, R. Rawls and M. S. El-Bayoumi, *Pure Appl. Chem.*, 1965, **11**, 371; (*b*) M. Kasha, in *Spectroscopy of the Excited State*, ed. B. D. Bartolo, Plenum, New York, 1976, pp. 337; (*c*) *Physical Processes in Radiation Biology*, ed. L. Augenstein, R. Mason, B. Rosenberg, Academic, New York, 1964, pp. 17.

21 (*a*) H. P. J. M. Dekkers, in *Circular Dichroism Principles and Applications*, ed. N. Berova, K. Nakanishi and R. W. Woody, Wiley-VCH, New York, 2000, pp. 185; (*b*) P. Salvadori and L. Di Bari, in *Chirality in Natural and Applied Science*, ed. W. J. Lough and I. W. Wainer, Blackwell, Oxford, 2002, pp. 215.